Hybrid lithography: Combining UV-exposure and two photon direct laser writing

Carsten Eschenbaum,* Daniel Großmann, Katja Dopf, Siegfried Kettlitz, Tobias Bocksrocker, Sebastian Valouch, and Uli Lemmer

Light Technology Institute and Institute for Microstructure Technology, Karlsruhe Institute of Technology, Engesserstr. 13, 76131 Karlsruhe, Germany

*carsten.eschenbaum@kit.edu

Abstract: We demonstrate a method for the combination of UV-lithography and direct laser writing using two-photon polymerization (2PP-DLW). First a dye doped photoresist is used for UV-lithography. Adding an undoped photoresist on top of the developed structures enables three-dimensional alignment of the 2PP-DLW structures by detecting the spatially varying fluorescence of the two photoresists. Using this approach we show three dimensional alignment by adding 3D structures made by 2PP-DLW to a previously UV-exposed structure. Furthermore, a fluidic system with an integrated total internal reflection mirror to observe particles in a microfluidic channel is demonstrated.

©2013 Optical Society of America

OCIS codes: (110.6895) Three-dimensional lithography; (110.3960) Microlithography; (220.3740) Lithography; (220.4000) Microstructure fabrication.

References and links

1. M. J. Madou, *Manufacturing Techniques for Microfabrication and Nanotechnology* (CRC, 2012).
2. C. M. Waits, A. Modafe, and R. Ghodssi, "Investigation of gray-scale technology for large area 3D silicon MEMS structures," J. Micromech. Microeng. **13**(2), 170–177 (2003).
3. W. Ehrfeld, "Recent developments in deep x-ray lithography," J. Vac. Sci. Technol. B **16**(6), 3526 (1998).
4. A. Neumeister, "Properties of three-dimensional precision objects fabricated by using laser based micro stereo lithography," J. Laser Micro. Nanoeng. **3**(2), 67–72 (2008).
5. A. Bertsch, P. Bernhard, C. Vogt, and P. Renaud, "Rapid prototyping of small size objects," Rapid Prototyping J. **6**(4), 259–266 (2000).
6. A. Bertsch, H. Lorenz, and P. Renaud, "3D microfabrication by combining microstereolithography and thick resist UV lithography," Sens. Actuators A **73**(1–2), 14–23 (1999).
7. S. Steen, S. J. McNab, L. Sekaric, I. Babich, J. Patel, J. Bucchignano, M. Rooks, D. M. Fried, A. W. Topol, J. R. Brancaccio, R. Yu, J. M. Hergenrother, J. P. Doyle, R. Nunes, R. G. Viswanathan, S. Purushothaman, and M. B. Rothwell, "Hybrid lithography: The marriage between optical and e-beam lithography. A method to study process integration and device performance for advanced device nodes," Microelectron. Eng. **83**(4–9), 754–761 (2006).
8. F. Romanato, R. Kumar, and E. Di Fabrizio, "Interface lithography: a hybrid lithographic approach for the fabrication of patterns embedded in three-dimensional structures," Nanotechnology **16**(1), 40–46 (2005).
9. M. Malinauskas, M. Farsari, A. Piskarskas, and S. Juodkazis, "Ultrafast laser nanostructuring of photopolymers: A decade of advances," Phys. Rep. **533**, 1–31 (2013).
10. S. Maruo, O. Nakamura, and S. Kawata, "Three-dimensional microfabrication with two-photon-absorbed photopolymerization," Opt. Lett. **22**(2), 132–134 (1997).
11. A. Ostendorf and B. N. Chichkov, "Two-photon polymerization: A new approach to micromachining," Photonics Spectra (2006).
12. O. P. Parida and B. Navakant, "Characterization of optical properties of SU-8 and fabrication of optical components," in *Int. Conf. on Opt. and Photon.(CSIO)* (2009), pp. 4–7.
13. B. J. Jung, H. J. Kong, B. G. Jeon, D.-Y. Yang, Y. Son, and K.-S. Lee, "Autofocusing method using fluorescence detection for precise two-photon nanofabrication," Opt. Express **19**(23), 22659–22668 (2011).
14. H. Wu, T. W. Odom, D. T. Chiu, and G. M. Whitesides, "Fabrication of complex three-dimensional microchannel systems in PDMS," J. Am. Chem. Soc. **125**(2), 554–559 (2003).
15. T. Woggon, T. Kleiner, M. Punke, and U. Lemmer, "Nanostructuring of organic-inorganic hybrid materials for distributed feedback laser resonators by two-photon polymerization," Opt. Express **17**(4), 2500–2507 (2009).
16. J. Serbin, A. Egbert, A. Ostendorf, B. N. Chichkov, R. Houbertz, G. Domann, J. Schulz, C. Cronauer, L. Fröhlich, and M. Popall, "Femtosecond laser-induced two-photon polymerization of inorganic-organic hybrid materials for applications in photonics," Opt. Lett. **28**(5), 301–303 (2003).

#199162 - $15.00 USD Received 14 Oct 2013; revised 15 Nov 2013; accepted 15 Nov 2013; published 26 Nov 2013

17. K.-S. Lee, R. H. Kim, D.-Y. Yang, and S. H. Park, “Advances in 3D nano/microfabrication using two-photon initiated polymerization,” Prog. Polym. Sci. **33**(6), 631–681 (2008).
18. M. Canva, G. Roger, F. Cassagne, Y. Lévy, A. Brun, F. Chaput, J.-P. Boilot, A. Rapaport, C. Heerdt, and M. Bass, “Dye-doped sol-gel materials for two-photon absorption induced fluorescence,” Opt. Mater. **18**(4), 391–396 (2002).
19. A. Fischer, C. Cremer, and E. H. Stelzer, “Fluorescence of coumarins and xanthenes after two-photon absorption with a pulsed titanium-sapphire laser,” Appl. Opt. **34**(12), 1989–2003 (1995).
20. C. Eggeling, A. Volkmer, and C. A. M. Seidel, “Molecular photobleaching kinetics of Rhodamine 6G by one- and two-photon induced confocal fluorescence microscopy,” ChemPhysChem **6**(5), 791–804 (2005).
21. S. W. Kettlitz, S. Valouch, W. Sittel, and U. Lemmer, “Flexible planar microfluidic chip employing a light emitting diode and a PIN-photodiode for portable flow cytometers,” Lab Chip **12**(1), 197–203 (2012).
22. H. Yamada, Y. Yoshida, and N. Terada, “Blood cell counter in gravity-driven microchannel,” Jpn. J. Appl. Phys. **44**(12), 8739–8741 (2005).
23. S. Inoué and K. R. Spring, *Video Microscopy: The Fundamentals* (Plenum, 1997), p. 741.
24. L. J. Guo, “Nanoimprint lithography: Methods and material requirements,” Adv. Mater. **19**(4), 495–513 (2007).

1. Introduction

The developments in optical lithography are of utmost importantance for the miniaturization of micro- and nanosystems [1]. The emerging requirement of 3D nano- and microstructures in different research fields have led to a variety of novel fabrication techniques. Nowadays, 3D structures are fabricated by a variety of lithographic techniques. Besides the classical layer-by-layer technique, gray-scale lithography has shown its potential for large area 3D MEMS microstructures [2]. X-ray lithography allows fabricating complex 3D structures using multiple exposure steps under different incident angles [3]. Micro-stereolithography is capable of fabricating complex microstructures [4,5]. Moreover this technology can be combined with thick resist UV-lithography [6], resulting in 3D microstructures. In addition to the above mentioned approaches a variety of hybrid lithography techniques combine electron-beam lithography with other techniques like X-ray or UV lithography [7,8]. Direct laser writing using two-photon polymerization (2PP-DLW) or avalanche ionization has shown its potential for the fabrication of complex three-dimensional nanostructures during the last decade [9–11]. However, all these techniques exhibit drawbacks. Either they are not suited for 3D nanofabrication, they suffer from their limited resolution, they are not suited for large scale patterning or they are extremely expensive or time-consuming.

In this paper we present a hybrid lithographic method suitable for the fabrication of 3D micro-and nanoscale devices by combining standard photolithography and 2PP-DLW. In the first step of this process, large scale structures are defined by UV-lithography into a dye doped photoresist. After developing these structures they are coated with undoped resist for 2PP-DLW. The strong luminescence of the dye doped structures is utilized to align both lithographic processes via the spatially varying fluorescence of the doped and undoped resist. Crosslinked and un-crosslinked SU-8 have very similar refractive indices [12], which makes it difficult to identify crosslinked SU-8-structures that have been coated with SU-8, as most of the techniques to identify the interface require a difference in the refractive index. Passive autofocus systems could detect the focal position with 1–2 µm precision for a standard flat sample [9]. For a non-flat interface the 3D resolution of 1 µm is acceptable. The direct observation of the appearance of the polymerized spot is not suitable to distinguish exposed and un-exposed SU-8 [13], as there is only a little difference in the fluorescence intensity and spectra. The alignment accuracy is determined by scanning across the vertical and horizontal interface between the doped and undoped photoresist. This method combines the advantages of standard lithography and 2PP-DLW. While the former is suited for large scale pattering, the latter technique enables to locally append three dimensional micro and nano-scale structures. Structures exposed by 2PP-DLW can either be connected to the lithographic pattern or they can be positioned independently with high accuracy. The resolution is only limited by the intrinsic resolution limit of the utilized lithographic methods.

In order to demonstrate the applicability of this method we present different examples where the 3D structure is written on top, at the sidewall or adjacent to an UV-exposed pattern. As an example for a microfluidic structure with an integrated 3D-optics, we fabricate a negative master of a microfluidic channel with an integrated total internal reflection (TIR)

mirror. Such a structure can easily be replicated by soft lithography [14]. In order to verify the functionality of our structure we use this optofluidic-system to measure the velocity profile of fluorescent particles across a fluidic channel.

2. Hybrid lithography

In Fig. 1 we illustrate the sequence of steps for the hybrid lithographic process. In the first step a 50 µm layer of SU-8 2050 (micro resist technology GmbH) containing rhodamine 6G (Sigma-Aldrich, 1 mg per 50 ml) is spin coated onto a 170 µm thick cover slip [Fig. 1(a)]. The subsequent softbake is conducted at 95°C on a contact hotplate for 9 min. The exposure dose is increased by a factor of two compared to undoped SU-8 [Fig. 1(b)], because of the additional absorption of the rhodamine 6G. The two step post exposure bake (PEB) following the UV-exposure is carried out at 65°C for 2 min and at 95°C for 7 min, respectively. Subsequently, the sample is developed for 7 min in MR-DEV 600 (micro resist technology GmbH). To ensure a complete crosslinking, the sample is hard baked at 130°C for 30 min.

In the second step, the sample is spin coated with an additional 80 µm thick layer of undoped SU-8 2050 [Fig. 1(d)], which is afterwards locally polymerized by 2PP-DLW using a setup described earlier [15]. The polymerization was induced by a focused femtosecond laser (Coherent Mira 900D titanium:sapphire laser). The laser has a central wavelength of 800 nm and emits 150 fs long pulses at a repetition rate of 76 MHz. A standard microscope (Zeiss Axioplan) and an oil immersion objective (Zeiss Apochromat 100x, N.A. 1.4) were used to focus into the photoresist. For the alignment of the structures, the difference in fluorescence of the two resists is observed through the CCD-camera of the 2PP-DLW-setup. 3D microstructures are thus added to the existing structures defined by UV lithography. The parameters used for writing are 1.3 mW laser power and 0.5 mm/s writing speed. The lateral separation of the voxel lines is 0.25 µm while the vertical distance is 0.5 µm. Following the second exposure step, PEB, development and hardbake are performed using the same parameters as in the UV-lithography step.

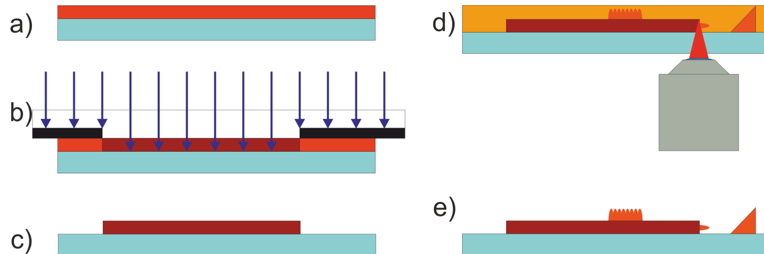

Fig. 1. Fabrication process of the hybrid lithography. (a) Glass cover slip spin coated with rhodamine 6G doped SU-8. (b) Microstructures definition by UV-lithography. (c) Developed 2D microstructures. (d) After coating with SU-8 2050, the 3D structures are written by 2PP. (e) Final 3D microstructure with 2PP-DLW structures shown in light red.

3. Lateral and vertical alignment

For the 3D alignment of the structures the contrast in fluorescence has to be detected. As seen in Fig. 2(a), slight difference in the emission spectra of the exposed and unexposed SU-8 can be observed. However, the intensity contrast is too low for a direct detection using a CCD-equipped microscope in the 2PP-DLW setup. Therefore, a fluorescent dopant was added to the resist in the first exposure step. For this rhodamine 6G doped SU-8 resist a much higher intensity is observed as shown in Fig. 2(a). The fluorescent dopant leads to an intensity one order of magnitude higher compared to the undoped resist.

To determine the alignment accuracy, the sample is scanned across the vertical and horizontal interface of the doped and undoped resist, respectively while the intensity is monitored in parallel. Therefore the fluorescence was excited by the femtosecond laser of the 2PP-DLW setup at a laser power one order of magnitude below the polymerization threshold.

#199162 - $15.00 USD Received 14 Oct 2013; revised 15 Nov 2013; accepted 15 Nov 2013; published 26 Nov 2013
(C) 2013 OSA

The different intensities of the unexposed SU-8 and the completely processed doped SU-8 measured with the CCD-camera are depicted in Figs. 2(c) and 2(d). Using this optical contrast, the interface between the doped and the undoped SU-8 can be easily determined.

Similar to the voxel size in 2PP-DLW [16,17], the axial height of the excited volume is a factor 2-4 bigger than the lateral size of the fluorescent volume. Therefore, the lateral alignment accuracy should be higher compared to the axial alignment. However, in both cases the accuracy was determined to be approximately 1 µm. The lateral alignment accuracy is slightly lower than expected because of the slope of the sidewall of the resist from the UV-lithographic step.

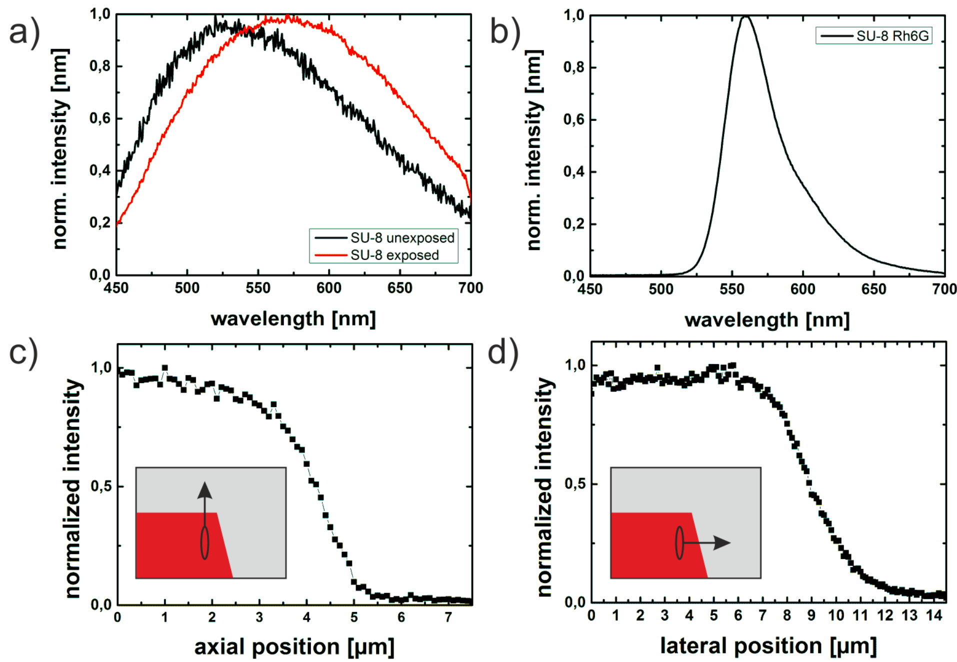

Fig. 2. (a) Comparison of exposed and unexposed spectra of SU-8. (b) Emission spectra of rhodamine 6G doped SU-8. (c) Axial intensity signal at the SU-8 rhodamine 6G interface (d) lateral intensity signal at the interface from the doped to the undoped SU-8 across the sloped sidewall. The insets depict the scanning of the voxel across the doped SU-8 interface.

Figure 3 shows three SEM images of different test structures. In Fig. 3(a) the logo of Light Technology Institute (LTI) was written onto the sidewall of a previously UV-exposed structure. Furthermore the logo was written on top of a large scale structure [Fig. 3(b)].

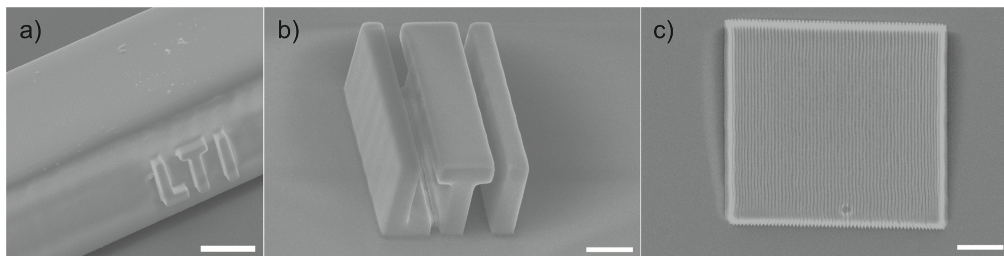

Fig. 3. Test structures for lateral and vertical alignment of 3D microstructures. (a) Logo attached at the sidewall of a UV-exposed structure (scale bar: 20 µm). (b) The logo written on top of a previously exposed structure (scale bar: 10 µm). (c) Grating written on top of a doped structure the grating period is 750nm (scale bar: 10 µm)

#199162 - $15.00 USD Received 14 Oct 2013; revised 15 Nov 2013; accepted 15 Nov 2013; published 26 Nov 2013
(C) 2013 OSA

An example for a facile combination of UV-lithography and submicron 2PP-DLW is shown in Fig. 3(c). The figure shows a nano-grating written on top of a previously patterned area. The grating has a period of 750 nm. We have observed that these structures written on top of a doped region require a higher exposure dose compared to freestanding structures. We attribute the higher required dose in the undoped SU-8 on top of the doped SU-8 to the higher attenuation of the DLW-beam by two-photon absorption in rhodamine 6G [18–20]. For the LTI-logo [Fig. 3(b)] the intensity of the laser was increased to 2.5 mW, while all other parameters were kept constant.

4. Microfluidic chip fabrication and characterization

2PP-DLW is a very interesting approach for rapid prototyping of master structures for soft lithography. The hybrid lithographic approach discussed here can also be used to fabricate a 3D master for soft lithography. In the following, we demonstrate a microfluidic device containing a total internal reflection mirror (TIR) close to a microfluidic channel to out-couple the fluorescence of particle within the channel. This device is a practical example for the benefits that arise from our hybrid lithography approach. As the size for the microfluidic system is 30 mm by 15 mm, writing the whole system by 2PP-DLW would be too time consuming and would exceed the range of a typical piezo-driven translation stage. Therefore the combination of 2PP-DLW with larger area UV-lithography is a promising approach for this field.

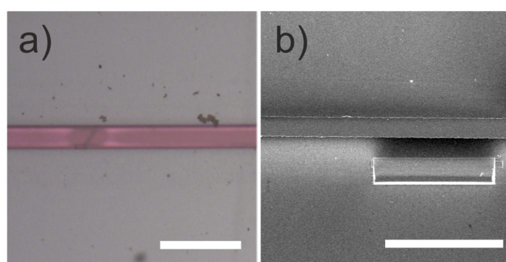

Fig. 4. (a) Optical micrograph of the microfluidic channel made out of rhodamine 6G doped SU-8 (scale bar: 200 µm) channel. (b) SEM image of the master including a 2PP-DLW written TIR-mirror in a distance of 35µm to the channel and a footprint of 50 µm by 250 µm and a height of 50 µm (scale bar: 250 µm).

Figure 4(a) shows the rhodamine doped SU-8 structure after UV-exposure and development. The cross-section of the channel was 50 µm x 50 µm. Afterwards the channel is covered with undoped SU-8 and the TIR-mirror is written via 2PP in a distance of 35 µm parallel to the channel. The TIR-mirror was written with a footprint of 50 µm by 250 µm and a height of 50 µm [Fig. 4(b)]. Therefore the reflecting face was tilted by 45 degrees. We use PDMS (Dow Corning, Sylgard 184 silicone elastomer kit) to replicate the master by soft lithography. A ratio of 10:1 base material to curing agent is mixed and degassed for 30 min under vacuum. The master is treated with hexamethyldisilazane (HMDS, Sigma-Aldrich) before pouring PDMS on the structures. The PDMS is cured at 100°C on a contact hot plate for 15 min. After removing the PDMS from the master the chip is sealed with a PMMA cover slip via the inherent adhesion of PDMS to PMMA. Employing this technique allows the fabrication of a microfluidic chip with integrated total internal reflection mirrors (TIR).

Observation of fluorescent particles (Kisker, PFP-6056, size: 6.0-7.9 µm) via the TIR-mirror is tested with an inverted microscope (Nikon Eclipse TE200-U) and a CMOS-camera (Canon EOS 550D). To excite the particles, a frequency doubled diode dumped solid state (DPSS) laser working at a wavelength of 532 nm (HB-Laserkomponenten GmbH, DPSS green 532/80) is focused via the microscope into the microfluidic channel. Excitation light is filtered by a longpassfilter (RU 532 LP, AHF Analysetechnik AG).

The refractive index of PDMS at a wavelength of 635 nm has a value of 1.42 [12], resulting in a total internal reflection angle of 44.86°. A major part of the fluorescence is therefore reflected by TIR. After fabrication, the whole fluidic system is filled with PBST

#199162 - $15.00 USD Received 14 Oct 2013; revised 15 Nov 2013; accepted 15 Nov 2013; published 26 Nov 2013
(C) 2013 OSA

(Sigma-Aldrich, phosphate buffered saline with Tween-20, 10 x concentrated) solution diluted 22:1:10 with fluorescent particles (Kisker, PFP-6056) and deionized water. This solution is used to match the specific density of the particles and thereby prevent them from sinking to the bottom of the channel [21]. This solution is then driven by gravity to achieve constant flow through the microfluidic channel [22].

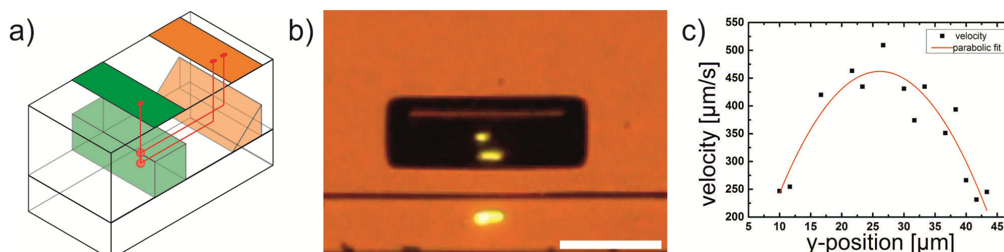

Fig. 5. (a) Schematic drawing of the channel (green) for two particles on top of each other with different z-positions. The red lines indicate the direct and reflected beampath of the particles. (b) The microscope image corresponds to the top view of the schematic drawing (scale bar 100 µm). (c) Velocity profile of fluorescent particles moving along the fluidic channel 6 µm above the bottom of the channel. The red line is a second order polynomial fit.

Figure 5(a) shows a schematic of the microfluidic channel and the TIR-mirror. A microscope image corresponding to the situation schematically shown in Fig. 5(a) is depicted in Fig. 5(b). Both particles have the same lateral position but different z-positions inside the fluidic channel. The TIR-mirror shows the two images of these particles, indicating their different z-position. This arrangement enables the simultaneous observation of particles inside a fluidic channel from two perpendicular directions resulting in the knowledge of the x-, y- and z-position of each particle. To overcome the blurring due to the limited depth of focus (DOF) of the microscope an objective with a low magnification (Nikon 4x/0.10) is used [23]. In this case the DOF is approximately 100 µm, which is sufficient to cover both, the direct image from the channel and the image reflected by the TIR-mirror. The integrated mirror can be used to map out the velocity profile across the complete microfluidic channel. As an example, Fig. 5(c) shows the measure velocity profile in a plane 6 µm above the bottom of the channel. The particle velocities are manually determined from the CMOS-images by extracting the propagation length over a time period of 40 ms.

5. Conclusion

We have developed a method for three dimensional alignment of patterns fabricated by a combination of conventional UV-lithography and 2PP-DLW. The resist used for UV-lithography is doped with a fluorescent dye. After developing the structures and covering the latter with a conventional resist, the doped structures could be identified through the contrast in fluorescence intensity. After UV-lithography of the larger structure, an aligned 2PP-DLW step allows to fabricate small 3D structures on or adjacent to the large structures. This hybrid lithography method is capable for the fabrication of complex 3D masters for different replication techniques in the field of microfluidics, photonics and MEMS. In particular photonic application might require a subsequent replication by nano imprint lithography or hot embossing to avoid fluorescence of the dye [24]. This method allows for easy and fast fabrication of large scale lithographic structures in combination with nano-scale and/or 3D structures. As a proof of concept, a master for soft-lithography was produced, which consists of a microfluidic-system in combination with a TIR-mirror. This optofluidic system enables three dimensional particle tracking inside a microfluidic channel.

Acknowledgments

We acknowledge the support by the Deutsche Forschungsgemeinschaft and Open Access Publishing Fund of Karlsruhe Institute of Technology. T. Bocksrocker acknowledges the support of Karlsruhe School of Optics & Photonics.